Memorias del 2023 Congreso Nacional de Control Automático
25-27 de Octubre, 2023. Acapulco, Guerrero, México.

From PID to Set Point Weighted PID: A Teaching DC-DC Buck Converter Platform ⋆

Luis Luna, Erick Asiain *
Luis Alberto Cantera-Cantera, Mario López-Pacheco **
A Gutierrez-Giles ***

* *CECyT 9-Instituto Politécnico Nacional, Mexico City, Mexico (e-mail: jlunap@ipn.mx, easiaind@ipn.mx).*
** *ESIME-Zacatenco Instituto Politécnico Nacional, Mexico City, Mexico (e-mail: lcantera@ipn.mx, mlaopezp@ipn.mx).*
*** *INAOE-Puebla City, Puebla (e-mail: alejandro.giles@inaoe.mx).*

Abstract: This article presents a lowcost educational platform based on a DC-DC Buck Converter to implement real-time control laws for engineering students. The motivation for this work arises from what happened during the COVID-19 pandemic when students did not have access to laboratory equipment and instruments necessary for their academic development. Particularly in the subjects of electrical circuits, electronics, and control, there has been a significant drop in the development of projects. This work shows the Buck converter's modeling and design to build and program different control laws like the Proportional Integral Derivative and the Setpoint weighted PID. Real-time experiments show the performance of the DC-DC Buck converter. The control algorithms are implemented using the MatLab / Simulink programming platform under the Waijung real-time control environment and an STM32704 data acquisition card.

Keywords: Control Education, DC-DC Buck Converter, PID, Setpoint weighted PID, Real time control systems.

1. INTRODUCTION

Social distancing is a situation that is likely to become a constant in the years to come. As a result of COVID-19, remote laboratories were emerging as a practical alternative to conventional laboratories and are gaining more attention due to the good results obtained by universities, especially in the engineering area [Martell-Chavez et al. (2023)]. Courses were to be redesigned to develop the projects using different software such as Fluid Sim, Raspberry Pi, LabVIEW, Arduino [Lyu and Zhang (2023)], MATLAB, Python, and others [Pires and Silva (2002); Chancharoen and Maneeratana (2020); Aliane (2009)]. Education in topics related to the Mechatronics area proposes virtual laboratories to evaluate topics like Microcontrollers, Robotics, Electrical Circuits, Power Electronics, and Automatic Control [Delgado et al. (2020)]. However, virtual laboratories limit the students only to these resources and may overlook issues like measurement noise in the data acquisition and disturbances which appear in real-life applications. A project poorly conceived that is too complicated or too advanced, given the students' knowledge and resources, will likely result in confusion that could lead to uncertainty in knowledge gained from the lectures and formal lab exercises.

The theory of engineering topics is most often taught with the help of a laboratory to let students connect theory with practice. Real-time prototypes allow the students direct interaction with a real system improving their programming skills to apply them in the Mechatronic area and other related topics [del Muro Alvarez et al. (2020), Maldonado Ramos et al. (2019)]. There exist prototypes based on a DC motor [Bernstein (2005)] that are suitable to this end, but their cost is too high.

The work done by [Tang and Xi (2020)] presents a low-cost platform for power electronics education. In turn, [Zhao (2022)] employs a DC-DC converter to carry out the motor speed control. Motivated by the above works, this paper presents a lowcost educational prototype based on a DC-DC buck converter which is an alternative to introducing students to problems related to modeling, design, building, programming, real-time implementation, noise measurements, and disturbances, taking into account students social and economic conditions.

⋆ The financial support given by SNI-CONAHCyT to the first, second, fourth and fifth authors is also recognized.

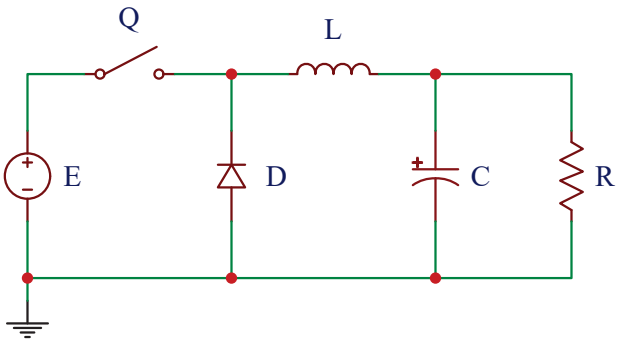

Fig. 1. DC-DC buck converter circuit diagram.

Another goal of this work is to explain and implement a Proportional Integral Derivative Control in a lowcost educational prototype based on a DC-DC buck converter and to show the viability of this device for testing advanced control laws. The Proportional Integral Derivative (PID) [Åström and Hägglund (2006)] control law is the most employed algorithm for regulating power converters [Samosir et al. (2023)], servos [Garrido and Luna (2018)], robot manipulators [Spong et al. (2020); Gutierrez-Giles et al. (2021)], and it is a relevant topic for mechatronics students to understand and introduce them to more complex algorithms.

The outline of this exposition is as follows. After introducing the basic mathematical model, the work describes how to design and select the appropriate components of a DC-DC buck converter applied to a teaching platform. Subsequently, the description and costs, software implementation, and connections are presented. Real-time experiments allow for assessing the performance of the educational platform controlled by the PID and a Set Point Weighted PID.

2. MATHEMATICAL MODEL

A DC-DC buck converter is a device whose average output voltage is less than the input voltage. Figure 1 shows a buck converter consisting of a switch Q, a diode D, an inductor I, a resistor R, a capacitor C, and a constant input voltage E.

The operation of the DC-DC buck converter can be divided into two modes. The first mode starts when the switch Q turns on. The input current rises and flows through the inductor, and the capacitor begins to charge. The second mode is when the switch Q is off or disconnected. The current stored in the inductor starts to flow through the diode and powers the load.

2.1 Mathematical model when the switch on $u = 1$

Figure 2 shows the two possible DC-DC buck converter configurations. The first is when the switch is on position $u = 1$. Using Kirchhoff's Voltage Law allows obtaining

$$E = V_L + V_C \tag{1}$$

where E is the voltage source amplitude, V_C and V_L are the capacitor and the inductor voltages, respectively. Equation (1) can be rewritten in terms of the inductor currents as follows

$$E = L\frac{di_L}{dt} + V_C \tag{2}$$

Now, applying Kirchhoff's Current Law produce

$$i_L = i_C + i_R \tag{3}$$

where

$$i_C = C\frac{dV_C}{dt} \tag{4}$$

and

$$i_R = \frac{V_C}{R} \tag{5}$$

Substituting (4) and (5) into (3) yields

$$C\frac{dV_C}{dt} = i_L - \frac{V_C}{R} \tag{6}$$

Therefore, from equations (2) and (6), the inductor current and the capacitor voltage are computed as

$$\frac{di_L}{dt} = \frac{1}{L}\left(E - V_C\right) \tag{7}$$

$$\frac{dV_C}{dt} = \frac{1}{C}\left(i_L - \frac{V_C}{R}\right) \tag{8}$$

The above equations allow obtaining the following state space expression for the DC-DC buck converter model when $u = 1$

$$\frac{d}{dt}\begin{bmatrix} i_L \\ V_C \end{bmatrix} = \begin{bmatrix} 0 & -\frac{1}{L} \\ \frac{1}{C} & -\frac{1}{RC} \end{bmatrix}\begin{bmatrix} i_L \\ V_C \end{bmatrix} + \begin{bmatrix} \frac{E}{L} \\ 0 \end{bmatrix} \tag{9}$$

2.2 Mathematical model when the switch on $u = 0$

The second configuration is when the switch is on off position $u = 0$, (see Fig. 2). Applying Kirchhoff's Voltage Law produces

$$V_C + V_L = 0 \tag{10}$$

The above equation can be rewritten in terms of the inductor current as follows

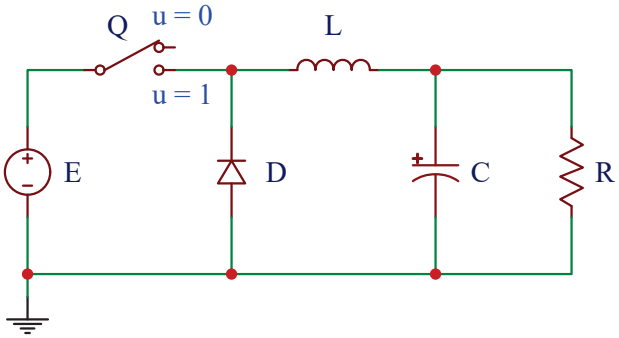

Fig. 2. DC-DC buck converter states.

$$V_C + L\frac{di_L}{dt} = 0 \tag{11}$$

From (11), it follows that

$$\frac{di_L}{dt} = -\frac{1}{L}V_C \tag{12}$$

Using Kirchhoff's Current Law thus leads to

$$i_L = C\frac{dV_C}{dt} + \frac{V_C}{R} \tag{13}$$

from which, it is not difficult to obtain

$$\frac{dV_C}{dt} = \frac{1}{C}\left(i_L - \frac{V_C}{R}\right) \tag{14}$$

Using (12) and (14) allows writing the state space expression for the DC-DC buck converter model when $u = 0$ as

$$\frac{d}{dt}\begin{bmatrix} i_L \\ V_C \end{bmatrix} = \begin{bmatrix} 0 & -\frac{1}{L} \\ \frac{1}{C} & -\frac{1}{RC} \end{bmatrix}\begin{bmatrix} i_L \\ V_C \end{bmatrix} \tag{15}$$

Finally, the average model combining (9) and (15) is given by

$$\frac{d}{dt}\begin{bmatrix} i_L \\ V_C \end{bmatrix} = \begin{bmatrix} 0 & -\frac{1}{L} \\ \frac{1}{C} & -\frac{1}{RC} \end{bmatrix}\begin{bmatrix} i_L \\ V_C \end{bmatrix} + \begin{bmatrix} \frac{E}{L} \\ 0 \end{bmatrix} u \tag{16}$$

where u is defined as

$$u = \{0, 1\} \tag{17}$$

3. TEACHING DC-DC BUCK CONVERTER PLATFORM

3.1 Design

For the design of the DC-DC buck converter [Batarseh and Harb (2018)], it is necessary to obtain the values of the resistance R, inductance L, and capacitance C from the following characteristics

- Input voltage $E = 12$ V.
- Output voltage $V_o = 6$ V.
- Switching frequency $f = 32$ kHz.
- Output power $P_o = 200$ mW.
- The ratio of the ripple to the output voltage

$$\frac{\Delta V_C}{V_o} = 1.5 \times 10^{-11}$$

.

The Duty Cycle D is given by

$$D = \frac{V_o}{E} = 0.5 \tag{18}$$

The value of the resistor R can be calculated as

$$R = \frac{(V_o)^2}{P_o} = 180\,\Omega \tag{19}$$

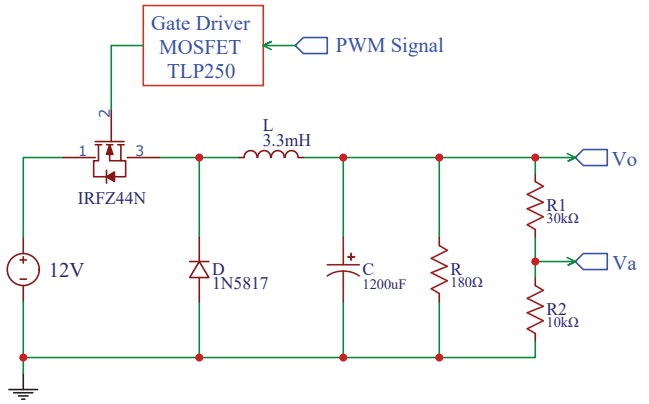

Fig. 3. Electrical diagram of the DC-DC buck converter.

The critic inductance value L_{cr} is calculated as

$$L_{cr} = \left(\frac{1-D}{2}\right)\left(\frac{R}{f}\right) = 1.4\,\text{mH} \tag{20}$$

The value L_{cr} must be multiplied by a factor with a magnitude equal to two to ensure a good performance of the platform, then

$$L = 2L_{cr} = 2.8\,\text{mH} \tag{21}$$

The commercial value for this case is $L = 3.3$ mH.

The capacitance value is performed as follows

$$C = \frac{1-D}{8Lf^2\left(\frac{\Delta V_C}{V_o}\right)} = 1233\,\mu\text{F} \tag{22}$$

The closest commercial value corresponds to $C = 1200$ μF.

3.2 Teaching platform

Fig. 4 depicts the teaching platform. It consists of a DC-DC buck converter, a TLP250 driver, an IRFZ44N MOSFET, and a voltage divider, see Fig. 3. A power supply of 24 V feeds the DC-DC buck converter, which has an LM7812, to obtain 12 V.

The STM32407 data acquisition card produces a 32 kHz PWM signal whose duty cycle depends on the control signal, which ranges from 0 to 100. This signal powers the TLP250 and the IRFZ44N. The voltage divider V_a feeds an analog input of the STM32407 to data acquisition. The algorithms are coded through MatLab/Simulink and Waijung real-time control software. A personal computer (Intel Core i7) executes the software. The Simulink diagrams utilize a sampling period of 1 ms and the Euler-ode1 integration method.

3.3 Costs

The components and their costs in American dollars are shown in Table 1.

The cost of the teaching prototype, including the power supply, is less than $50 US. This price could be decreased

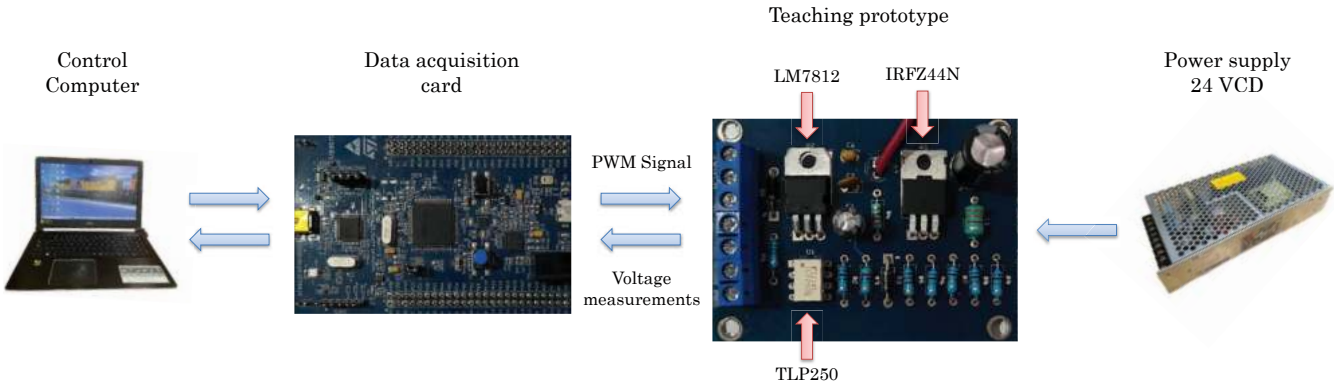

Fig. 4. Teaching platform experimental setup.

Table 1. Components cost.

Component	Cost
LM7812	$0.57
1N4005 Diode	$0.05
1200 μF Electrolytic capacitor	$0.37
180 Ω Resistance	$0.05
10 kΩ Resistance	$0.05
30 kΩ Resistance	$0.2
3.3 mH Inductor	$0.45
TLP250	$2.96
IRFZ44N MOSFET	$1.42
1N5817 Schottky diode	$0.17
STM32407	$21.17
24 V Power supply	$18.99
Total	$46.45

by buying the electronics components in large amounts. The low cost and portability of the prototype make it viable to employ it in the classroom or for personal learning.

4. PID AND SET POINT WEIGHTED PID CONTROL

4.1 Proportional Integral Derivative Control

The PID controller has been at the heart of control engineering practice for nearly a century. The ability of PID controllers to regulate most practical processes has led to their widespread acceptance in industrial applications. The structure of an ideal PID controller with error response is [Åström and Hägglund (1995)]:

$$u = \underbrace{K_p e}_{\text{Proportional action}} + \underbrace{K_i \int_0^t e(\tau)d\tau}_{\text{Integral action}} + \underbrace{K_d \frac{d(e)}{dt}}_{\text{Derivative action}} \tag{23}$$

where K_p is the proportional gain, K_i is the integral gain and K_d is the derivative gain. The error is defined as $e := r - y$; the signal r is called the reference and the signal y is the measured output of the process to be controlled. The PID control law consists of applying the sum of three types of control actions: A proportional action, an integral action, and a derivative action. While the proportional action is based on the current value of the error and the integral action uses the past values of the error, the derivative action is proportional to the error derivative e. However, it has some issues that make it not widely adopted in use cases. In fact, the use of high gains in the pure derivative action is responsible for the amplification of measurement noise. In practice, a very noisy signal from the control variable could cause damage to the actuator. The problems described above can be solved by filtering the derivative action. The filter time constant must be selected to adequately filter noise while preventing the poor performance of the PID controller. Another issue related to the derivative action is that when there is a sudden change of the reference signal r, the derivative action takes high values and results in an overshoot and a spike in the control signal, which is undesirable and it can cause saturation of the actuators. A simple solution to avoid this problem is to apply the derivative term only to the output of the process [Visioli (2006)].

Then, the control law (23) is transformed into the equation (24):

$$u = K_p e + K_i \int_0^t e(\tau)d\tau - K_d \frac{dy(t)}{dt} \tag{24}$$

4.2 Set Point Weighted PID (WPID)

A more flexible structure according to [Åström and Hägglund (1995)] and [Visioli (2006)] is obtained by treating the reference and the process output separately. A PID controller of this form is given by

$$u = K_p e_p + K_i \int_0^t e(s)ds + K_d \frac{de_d}{dt} \tag{25}$$

where the error in the proportional part is defined as $e_p = \hat{b}r - y$, in the derivative part it corresponds to $e_d = cr - y$ and the constant weights are defined with the letters $\hat{b}$ and c. The error in the integral part is $e = r - y$ in order to avoid steady-state errors. This type of structure with the weighting of the set point is proposed in [Hägglund and Åström (1985)], where the weights in the error of the proportional and derivative part are weighted with values between 0 and 1 [Taguchi and Araki (2000)].

An advantage of this type of configuration is that by making an appropriate choice of the weight at the set point for the proportional action, the overshoot in the system response is reduced, improving its performance [Visioli (2012)].

5. REAL TIME EXPERIMENTS

The educational platform and the PID controller studied in Section 4 is experimentally assessed. Several weights for $\hat{b}$ are tested to show the performance of the set point weighted PID control scheme. The performance of the closed-loop system is evaluated through the Integral Squared Error (ISE), the Integral of the Absolute value of the Error (IAE), and the Integral of the Absolute value of the Control Variation ($IACV$) indexes that are defined as

$$ISE = \int_0^5 100\,[e]^2\,dt \qquad IAE = \int_{25}^{30} 100\,|e|\,dt$$

$$IACV = \int_0^{30} \left|\frac{du}{dt}\right| dt$$

The closed-loop responses, the control signals, and error graphs are depicted in Fig. 5, Fig. 6 and Fig. 7, respectively.

For this set of experiments, note that using $\hat{b} = 1$ and c=0, the structure of the PID controller given by (24) is

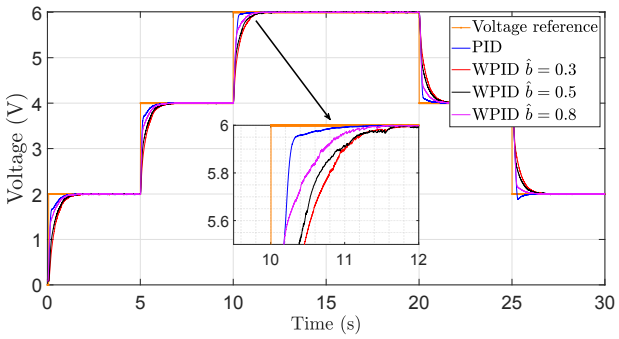

Fig. 5. Voltage responses.

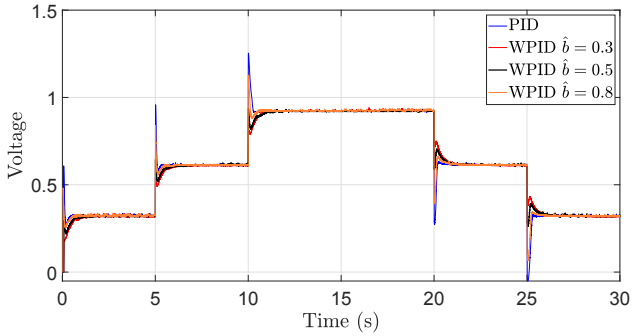

Fig. 6. Control signals.

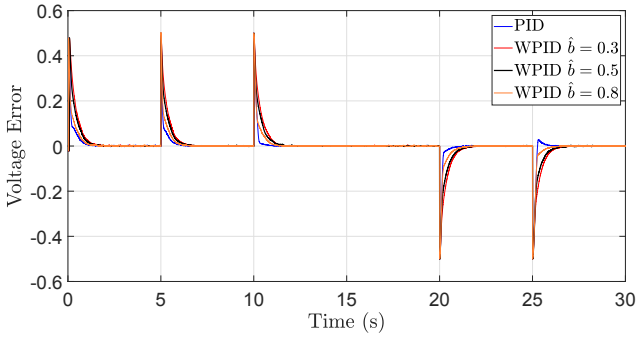

Fig. 7. Error signals.

Table 2. Experimental results using $K_p = 3$, $K_d = 10$ and K_I=10 for the PID controller.

$\hat{b}$	ISE	IAE	$IACV$
1	124.139	8.107	36.409
0.8	178.716	9.002	33.850
0.5	293.907	13.074	37.061
0.3	394.240	15.647	36.502

obtained. The gains values used are the same for all the experiments; the only parameter changed is the value of the weight $\hat{b}$.

According to Table 2, the ISE index that measures the error in the transient response is lower when using $\hat{b} = 1$ and $\hat{b} = 0.8$; as the weight value in the controller decreases, the performance degrades, and the response is slow. On the other hand, the IAE index that measures the error in a steady state in the last seconds of the experiment shows relative values for all values of $\hat{b}$. However, the slightest error in a steady state is when the PID control is used without weighing the reference.

Finally, the variation of the control signal is minor when using $\hat{b} = 0.8$, this suggests that setting the reference helps to reduce the variations in the control signal, and as can be seen in Fig. 5, the fact of weighting helps to eliminate the overshoots that are displayed during the 25th to 30th second. This suggests that to eliminate oscillations in the response and have an excellent steady-state response, values close to 1 should be used; if values less than 0.5 are used, performance degrades even though the system works reasonably.

6. CONCLUSIONS

The present paper describes a lowcost educational platform for teaching electronics, microcontrollers, and topics related to mechatronics as an alternative after the Covid-19 pandemic to ensure the quality of theoretical, practical, and laboratory lectures and to enhance modeling, programming, and hardware implementation skills.

It is important to mention that this platform, compared with Arduino kits, is cheaper, which makes it easier for students to acquire. In addition, the Waijung software,

being freely accessible, allows one to view the signals in real-time, using block programming that makes it easy to understand.

In future work, implementing nonlinear controllers, state observers, parametric identification by neural networks, algorithms such as orthogonal least squares, and evaluating the prototype through practices aimed at undergraduate and postgraduate students is contemplated.

ACKNOWLEDGEMENTS

Luis Luna and Erick Asiain want to thank the support of Martha Hernandez, Edgar Ramirez, and Natisma Lopez from CECyT 9-IPN. The work of Luis Cantera, Mario Lopez Pacheco, Luis Luna, Erick Asiain and Alejandro Gutierrez Giles were supported by National Research System (SNI) scholarships from CONAHCyT-MEXICO.

REFERENCES

Aliane, N. (2009). A matlab/simulink-based interactive module for servo systems learning. *IEEE Transactions on Education*, 53(2), 265–271.

Åström, K.J. and Hägglund, T. (2006). Pid control. *IEEE Control Systems Magazine*, 1066.

Åström, K.J. and Hägglund, T. (1995). *PID controllers: theory, design, and tuning*, volume 2. Isa Research Triangle Park, NC.

Batarseh, I. and Harb, A. (2018). Power electronics. In *Springer Nature*. Springer.

Bernstein, D.S. (2005). The quanser dc motor control trainer individual or team learning for hands-on control education-product review. *IEEE Control Systems Magazine*, 25(3), 90–93.

Chancharoen, R. and Maneeratana, K. (2020). Introducing raspberry pi and its peripherals to a mechatronics course under covid-19 disruption. In *2020 IEEE International Conference on Teaching, Assessment, and Learning for Engineering (TALE)*, 883–888. IEEE.

del Muro Alvarez, S., Delgado, L.D.R., and Gutiérrez, S. (2020). Mechatronics class through virtual platforms under covid-19. In *2020 IEEE International Conference on Engineering Veracruz (ICEV)*, 1–5. IEEE.

Delgado, L.D.R., del Muro Alvarez, S., Gutiérrez, S., and Ponce, H. (2020). Mechatronics teaching through virtual platforms for home confinement due to covid-19. In *2020 International Conference on Mechatronics, Electronics and Automotive Engineering (ICMEAE)*, 180–185. IEEE.

Garrido, R. and Luna, J.L. (2018). On the equivalence between pd+ dob and pid controllers applied to servo drives. *IFAC-PapersOnLine*, 51(4), 95–100.

Gutierrez-Giles, A., Evangelista-Hernandez, L.U., Arteaga, M.A., Cruz-Villar, C.A., and Rodriguez-Angeles, A. (2021). A force/motion control approach based on trajectory planning for industrial robots with closed control architecture. *IEEE Access*, 9, 80728–80740.

Hägglund, T. and Åström, K.J. (1985). Automatic tuning of pid controllers based on dominant pole design. *IFAC Proceedings Volumes*, 18(15), 205–210.

Lyu, S. and Zhang, Y. (2023). The analysis of dcdc buck circuit based on arduino. *Highlights in Science, Engineering and Technology*, 39, 536–544.

Maldonado Ramos, J.J., Luna Pineda, J.L., Garrido Moctezuma, R.A., and Castro Zavala, J.G. (2019). A teaching methodology based on an educational experimental platform. *IEEE Latin America Transactions*, 17(08), 1363–1370. doi: 10.1109/TLA.2019.8932370.

Martell-Chavez, F., López-Téllez, J.M., Paredes-Orta, C.A., and Espinosa-Luna, R. (2023). Virtual laboratories for teaching automation, robotics, and optomechatronics. In *2023 IEEE World Engineering Education Conference (EDUNINE)*, 1–4. IEEE.

Pires, V. and Silva, J. (2002). Teaching nonlinear modeling, simulation, and control of electronic power converters using matlab/simulink. *IEEE Transactions on Education*, 45(3), 253–261. doi:10.1109/TE.2002.1024618.

Samosir, A.S., Sutikno, T., and Mardiyah, L. (2023). Simple formula for designing the pid controller of a dc-dc buck converter. *International Journal of Power Electronics and Drive Systems*, 14(1), 327.

Spong, M.W., Hutchinson, S., and Vidyasagar, M. (2020). *Robot modeling and control*. John Wiley & Sons.

Taguchi, H. and Araki, M. (2000). Two-degree-of-freedom pid controllers—their functions and optimal tuning. *IFAC Proceedings Volumes*, 33(4), 91–96.

Tang, X. and Xi, Y. (2020). Application of hardware-in-loop in teaching power electronic course based on a low-cost platform. *Computer Applications in Engineering Education*, 28(4), 965–978.

Visioli, A. (2006). *Practical PID control*. Springer Science & Business Media.

Visioli, A. (2012). Research trends for pid controllers. *Acta Polytechnica*, 52(5).

Zhao, G. (2022). Research on teaching effect of power electronics experiment simulating engineering application system. *IET Power Electronics*, 15(16), 1956–1963.